Original article

Mechanistic analysis of A46V, H57Y, and D129N in pyrazinamidase associated with pyrazinamide resistance

Muhammad Tahir Khan [a], Sathishkumar Chinnasamy [b], Zhilei Cui [d], Muhammad Irfan [e], Dong-Qing Wei [b,c,*]

[a] Department of Bioinformatics and Biosciences, Capital University of Science and Technology, Pakistan
[b] State Key Laboratory of Microbial Metabolism, School of Life Sciences and Biotechnology, and Joint Laboratory of International Cooperation in Metabolic and Developmental Sciences, Ministry of Education, Shanghai Jiao Tong University, Shanghai 200240, China
[c] Peng Cheng Laboratory, Vanke Cloud City Phase I Building 8, Xili Street, Nanshan District, Shenzhen, Guangdong 518055, China
[d] Department of Respiratory Medicine, XinHua Hospital Affiliated to Shanghai Jiao Tong University School of Medicine, China
[e] Department of Microbiology and Cell Science, Genetics Institute and Institute of Food and Agricultural Sciences, University of Florida, Gainesville, FL, USA

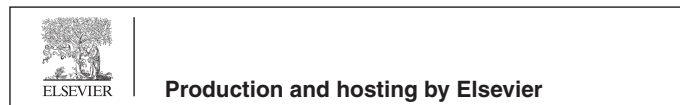## ARTICLE INFO

ABSTRACT

Pyrazinamide (PZA) is a component of first-line drugs, active against latent *Mycobacterium tuberculosis* (MTB) isolates. The prodrug is activated into the active form, pyrazinoic acid (POA) via *pncA* gene-encoded pyrazinamidase (PZase). Mutations in *pncA* have been reported, most commonly responsible for PZA-resistance in more than 70% of the resistant cases. In our previous study, we detected many mutations in PZase among PZA-resistance MTB isolates including A46V, H71Y, and D129N. The current study was aimed to investigate the molecular mechanism of PZA-resistance behind mutants (MTs) A46V, H71Y, and D129N in comparison with the wild type (WT) through molecular dynamic (MD) simulation. MTB positive samples were subjected to PZA drug susceptibility testing (DST) against critical concentration (100ug/ml). The resistant samples were subjected to *pncA* sequencing. Thirty-six various mutations have been observed in the coding region of *pncA* of PZA-resistant isolates (GenBank accession No. MH461111) including A46V, H71Y, and D129N. The post-simulation analysis revealed a significant variation in MTs structural dynamics as compared to the WT. Root means square deviations (RMSD) and Root means square fluctuation (RMSF) has been found in variation between WT and MTs. Folding effect and pocket volume were altered in MTs when compared with WT. Geometric matching supports the effect of mutation A46V, H71Y, and D129N on PZase structure that may have an insight effect on PZase dynamics, making them vulnerable to convert pro-PZA into active form, POA. In conclusion, the current analyses will provide useful information behind PZA-resistance for better management of drug-resistant TB.

© 2020 The Author(s). Published by Elsevier B.V. on behalf of King Saud University. This is an open access article under the CC BY-NC-ND license (http://creativecommons.org/licenses/by-nc-nd/4.0/).

1. Introduction

Pyrazinamide (PZA) is the only drug that kills *Mycobacterium tuberculosis* (MTB) in a latent state which has been successfully reduced the period of TB therapy from 9 to 6 months (Yadon et al., 2017). According to the World Health Organization report 2018, 23% of the world's population (1.7 billion) are infected with latent tuberculosis (TB) [W.H.O]. PZA is a prodrug that depends on MTB encoded, pyrazinamidase (PZase) activity for conversion into pyrazinoic acid (POA), an active form of PZA, targeting the trans-translation (Lu et al., 2011; Ying et al., 2003) process of ribosomal protein S1 (RpsA), where POA is disrupting the RpsA-tmRNA complex formation in MTB (Simons et al., 2013; Sørensen et al., 1998; Tan et al., 2014; Yang et al., 2015), that has potential effects on the persistent forms of MTB (Njire et al., 2016; Stehr et al., 2015). PZA resistance is associated with mutations in multiple target genes,

Production and hosting by Elsevier

including *pncA, rpsA,* and *panD.* However, mutations in *pncA* are the major mechanism of resistance in 70–97% cases with an average 85% resistance in MTB isolates (Akhmetova et al., 2015; Alexander et al., 2013; Khan et al., 2018b, 2018c; Zhang et al., 2013). PZase consists of four α-helices and six parallel β-sheets. The metal ion, Fe^{2+} ion, is surrounded by one aspartate (Asp49) and three histidines, His51, His57 and His71. The amino acids residues, Asp8, F13, L19, V21, D49, W68, H71, F94, Y95, Lys96, Y103, I133, A134, H137, and C138 have been found present in the catalytic site and its surroundings (Du et al., 2001; Petrella et al., 2011). Genetic mutations frequently affect the electrostatic nature of the target protein surface and the changes may affect the molecular dynamics, resulting in the loss of drug binding affinity (Aggarwal et al., 2017; Anand, 2018; Durairaj and Shanmughavel, 2019; Haq et al., 2012; Ma et al., 2003). Identification and analysis of mutations in the drug resistance MTB strains might be helpful to uncover molecular mechanisms underlying for better management of resistant TB.

Three major regions (amino acids 3 to 17, 61 to 85, and 132 to 142) of *pncA* are most commonly affected by mutations associated with changes in the PZase catalytic activity (Lemaitre et al., 2001; Sheen et al., 2009). However, Yoon et al. reported that mutations occurred at far from the active site may affect protein activity by altering the expression levels or protein folding (Yoon, Nam, Kim, & Ro, 2014). Protein structure may have drastic effects due to an amino acid substitution, altering the protein structure and function, especially the active site or binding pockets (Ganesan and Ramalingam, 2018; Worth et al., 2009). The mutation may also have effects in a long-range position (Kosloff and Kolodny, 2008). Exploring the mechanism of changes that occur behind a mutation is required for better understanding, however, these are time-consuming analyses and very expensive to address by experimental procedure alone.

Molecular dynamic (MD) simulations have been applied widely in exploring the mechanisms of conformational changes in protein, especially in drug resistance mechanisms caused by mutations. MD simulation studies of ligand–protein interactions are widely applied approach for explaining the mechanisms of drug resistance due to mutations, especially in the target protein. During *in vivo* analysis, the crystal structure is analyzed for drug resistance. However, it can be formed based on some experimental conditions where every protein-drug complex does not provide the mechanism of resistance, neither every structure can be attained by single-crystal X-ray diffraction.

In our recent studies, we have performed PZA drug susceptibility testing followed by the sequencing of the *pncA* and *rpsA* genes in which we identified some novel mutations that were associated with PZA-resistance (Khan et al., 2019a, 2019b; Khan et al., 2018c). MD simulation of some MTs in comparison with WT have been investigated for the mechanism behind resistance (Junaid et al., 2018; Khan et al., 2019a, 2019b, 2018d, 2018a; Rehman et al., 2019). Mutations in drug target proteins may cause changes in proteins' dynamic behavior which ultimately causing drug resistance. In the present study, we aimed to analyze the structural changes that occur in PZase behind mutations A46V, H71Y, and D129N in comparison with WT. We hypothesized that these mutations may affect the PZase structural dynamics that result in weak interaction with PZA, causing PZA-resistance. To test our hypothesis, we performed molecular dynamics simulations of MTs and WT PZase to study and compare the behavior of effect of mutation on proteins.

2. Material and methods

2.1. Study sample

The samples taken from TB patients were handled at the BSL-III facility of PTRL, Hayatabad Medical Complex (HMC). This laboratory accepts TB cases from the entire KP province where the mycobacterium growth indicator tube (MGIT) 960 system is used for testing the drug susceptibility.

2.2. Sample processing, isolation, and mycobacterial culture

To process these samples, the N-acetyl-L-cysteine–sodium hydroxide (NALC–NaOH) concentration technique (Kubica et al., 1963) was used. An equal amount of NaOH/N-acetyl-L-cysteine (NALC-NaOH) was added in a falcon tube containing a sample. This whole setup was incubated for 15 min to be decontaminated and digested. Lowenstein–Jensen medium (LJ) and MGIT tubes containing 7H9 media were used for culturing the suspect's samples.

2.3. Drug susceptibility testing (DST)

The automated BACTEC MGIT 960 system (BD Diagnostic Systems, NJ, USA) (Siddiqi and Gerdes, 2006), was used to test the PZA drug susceptibility. The *Mycobacterium tuberculosis* H37Rv and Mycobacterium bovis were used as controls, respectively. All the samples were labeled as PZA-resistant if growth has been detected at 100 µg/ml of the PZA critical concentration. This process was repeated several times to confirm the PZA resistance.

2.4. DNA extraction and PCR amplification of PZA-resistant samples

All the PZA-resistant samples were subjected to genomic DNA extraction via sonication (Buck et al., 1992; Kirschner et al., 1993). The Mycobacterium Growth Indicator Tube (MGIT) that contained a fresh culture from which 1 µL was taken and transferred to a microcentrifuge tube. An Echotherm™ IC22 Digital was used for boiling purposes at 86 °C for 30 min. Sonication was carried out for 15 min via ELMASONIC S30 Sonicator. The previously reported primers (*pncA*-F = 5GCGTCATGGACCCTATATC-3 and *pncA*-R = 5 AACAGTTCATCCCGGTTC-3 =) (Davies et al., 2000) were used for the amplification of fragments containing *pncA*. PCR reaction was performed as described in a previous study (Khan et al., 2019a, 2019b) These amplified PCR samples were sent to 6 Applied Biosystems 3730 xl (Macrogen Korea) for sequencing.

2.5. Sequenced pncA

The Mutation Surveyor V5.0.1 software [42] was applied to analyze the sequenced data in comparison with RefSeq (Rv2043c) of NCBI (NC_000962).

2.6. Data mining and preparation

The 3D crystallographic structure for MTB PZase was obtained from the Brookhaven Raster Display Protein Data Bank (PDB) by typing 3PL1 (Berman, 2008). All the water molecules were removed and mutations were inserted at A46V and H71Y using PyMOL (L DeLano, 2002).

The PubChem [48], an online database for chemical compounds was accessed to obtain the 3D chemical structure of PZA drug (PubChem CID: 1046) (Bolton et al., 2008). PubChem is hosted by the National Institutes of Health (NIH), storing and sharing chemical structures. The Chimera software package (Pettersen et al., 2004) was used for the energy minimization of protein-drug complexes before simulation.

2.7. Molecular docking and binding pocket analysis

The PatchDock server [51] was used to dock the WT and MTs with PZA to observe the impact of mutations on the protein-drug interactions. PatchDock measures the geometric features of a

ligand and receptor. The protein complexes which maintain good interactions usually exhibit better shape complementarity. Binding pockets of WT and MTs were measured through the online server, Computed Atlas Surface Topography of proteins (CASTp) [53]. The server measures a curved surface area that is suppressed inside the receptors. It also calculates the total surface volume.

2.8. Validation via molecular dynamics (MD) simulation

In comparison with the experimental approach, MD simulation has a particular advantage of exploring the mechanisms of drug resistance at the molecular level (Liu and Yao, 2010). Furthermore, the structural dynamics of protein complexes and other residues level information can be accessed which have been considered difficult by experimental procedures (Ding et al., 2013; Hou et al., 2008; M. Kalim A. Khan et al., 2018; Xue et al., 2012).

The wild type and mutant type of the proteins were performed by molecular dynamics (MD) simulation studies using GROMACS 5.1.2 package, (Berendsen et al., 1995) with GROMS96 53a6 force field. The topology of the protein was prepared by using Pdb2gmx. PRODRG server was used for initial ligand topology. The simple point charge (SPC) water model was solved to satisfy the electroneutrality of the system and protein was centered in a cubic box (Wu et al., 2006). The system was energy minimized by using the steepest descent algorithm and neutralized by Na^+ counterions. Restraining simulation of the position was employed to equilibrate the ions and solvent around the protein before the actual simulation. A constant number of atoms, volume, pressure, and temperature (NPT and NVT) ensembles were applied to the system for the MD simulation studies. Particle Mesh Ewald (PME) algorithm was used to calculate the long-range electrostatic interactions. Bond constraints of LINCS algorithms were applied to the system. The pressure of the system was embraced using the Parrinello–Rahman method and the temperature was regulated using the V-rescale method. Short-range Coulomb and Van der Waals interactions were set for cutoff values. Periodic boundary conditions were applied in all three dimensions. A total of 100 ns of MD simulation has been performed for the protein–ligand complex to analyze the behavior of WT and MTs complexes. The resulting structural coordinates were saved at every 2 ps of an interval.

3. Results

3.1. MTB culture result

A total of 4518 TB suspect samples were obtained and processed, among which 753 (16.6%) samples were detected as culture-positive (MTB). All the positive samples were subjected to PZA drug susceptibility testing for screening of PZA resistance MTB isolates.

3.2. PZA susceptibility pattern

Out of 753 MTB positive samples, 69 (14.8%) were detected as PZA resistant isolates. To find the role of *pncA* mutations in PZA-resistance, all the resistant MTB samples along with 26 PZA-

sensitive and one MTB H37Rv as control were sequenced to screen for the mutations in the coding region (561 bp) of *pncA* (PZase).

3.3. Screening of mutation in pncA and PZA resistance

Among the 69 PZA-resistant isolates, 51 (74%) has thirty-six different mutations in *pncA* gene (GeneBank Accession No. MH461111) including A46V, H71Y, and D129N. We did not detect mutations in sensitive isolates, except a synonymous mutation, 195C > T (Ser65Ser).

To explore the in-depth molecular mechanism behind resistance and mutations at position, A46V, and H4Y of PZase, multiple factors were investigated for better understanding of the mechanism behind PZA-resistance.

3.4. Binding pocket calculation of WT and mutant PZase

Any changes in the binding pockets may highly affect the linkage formation with a ligand, particularly a drug. The CASTp online tool analyzed the binding pocket to gauge the indirect effect of mutations on the structure. The pocket volume in the case of WT PZase is 585.736 Å, considered optimum for the PZA drug binding. Any deviation from this volume may impede the binding affinity. The binding pockets volume of MTs was compared with that of the WT, revealing significant changes (Table 1).

3.5. Proteins-ligand interactions

To form a strong bond between receptor and a ligand, various forms of interactions such as hydrogen and hydrophobic linkages are vital. The WT formed interactions with Ala 8, Ala 134, Ile133, and Cys 138. These observations confirm the PatchDock score as WT score higher than the MTs (Table 1). The 3D interactions of all the docked complexes are illustrated in Fig. 1.

3.6. Protein trajectory analysis

MD simulation of both the WT and MTs was performed on a high-performance cluster in a complex with the PZase drug for a duration of 100 ns to analyze the conformational changes caused by A46V and H4Y. The trajectories for MTs along with a WT were compared and carefully examined. WT exhibited RMSD between o.15 nm and 0.3 nm and remains fairly consistent at 100 ns (Fig. 2).

On the other hand, MTs attained a significant difference in their overall stability. MTs A46V and H71Y exhibited RMSD between 0.3 and 0.4, 0.15, and (Fig. 2) remains higher as compared to the WT.

The RMSF exhibited by MTs is higher than the WT (Fig. 3). The WT RMSF value ranges from 0.2 to 0.45 nm. The highest RMSF has been noted at the position between residue 90 and 100 reaching up to 0.9 nm. The graphical representation shows that the highest fluctuations occurred in between the residue 50 and 100, are much higher in MTs as compared to the WT.

A stable folding is essential for enzymes catalytic activity. The stability of protein structure folding in MD simulation is measured through a graph called a radius of gyration (Rg), plotted against the time (Fig. 4). The insights into the overall dimensions of folding
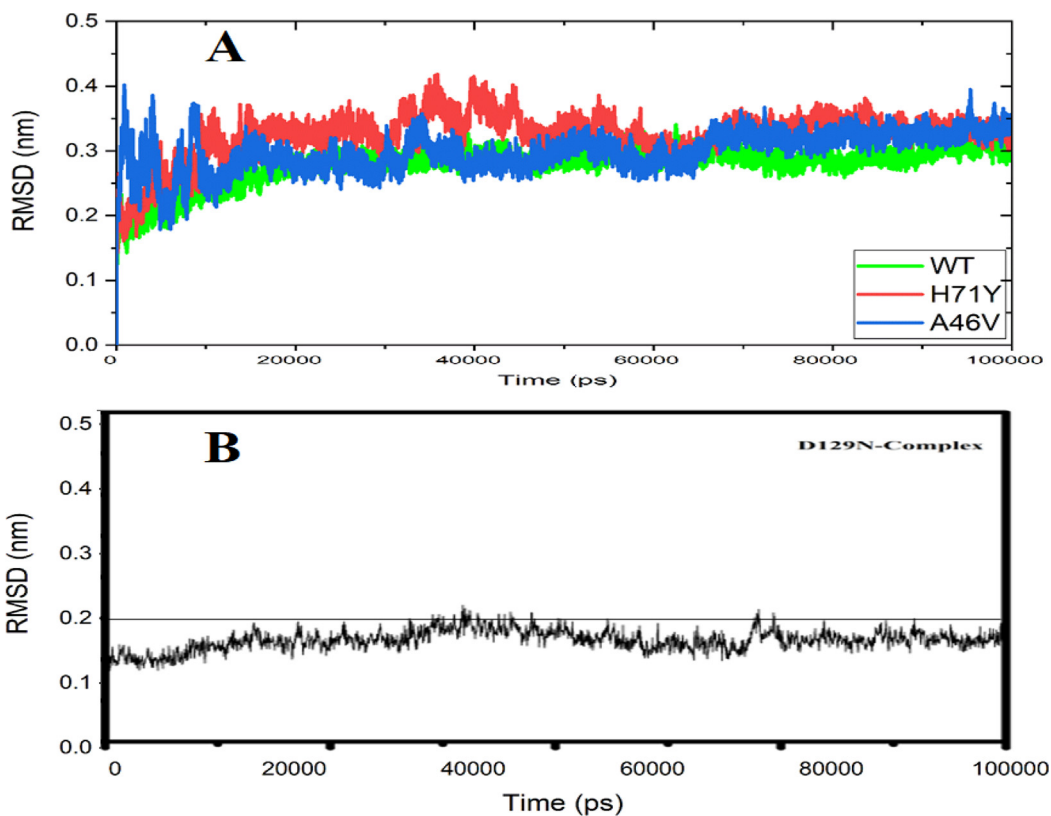
Table 1
Characteristics of WT and MTs PZase structures.

PZase Mutations	Cre-Conc[*] of PZA	DST result	PatchDock score	Pocket Volume (Å)
WT	100 µg/ml	Sensitive	2386	525.641 Å
A46V	100 µg/ml	Resistant	2382	525.641 Å
H71Y	100 µg/ml	Resistant	2382	333.695 Å
D129N	100 µg/ml	Resistant	2420	481.240 Å

[*] Critical concentration.
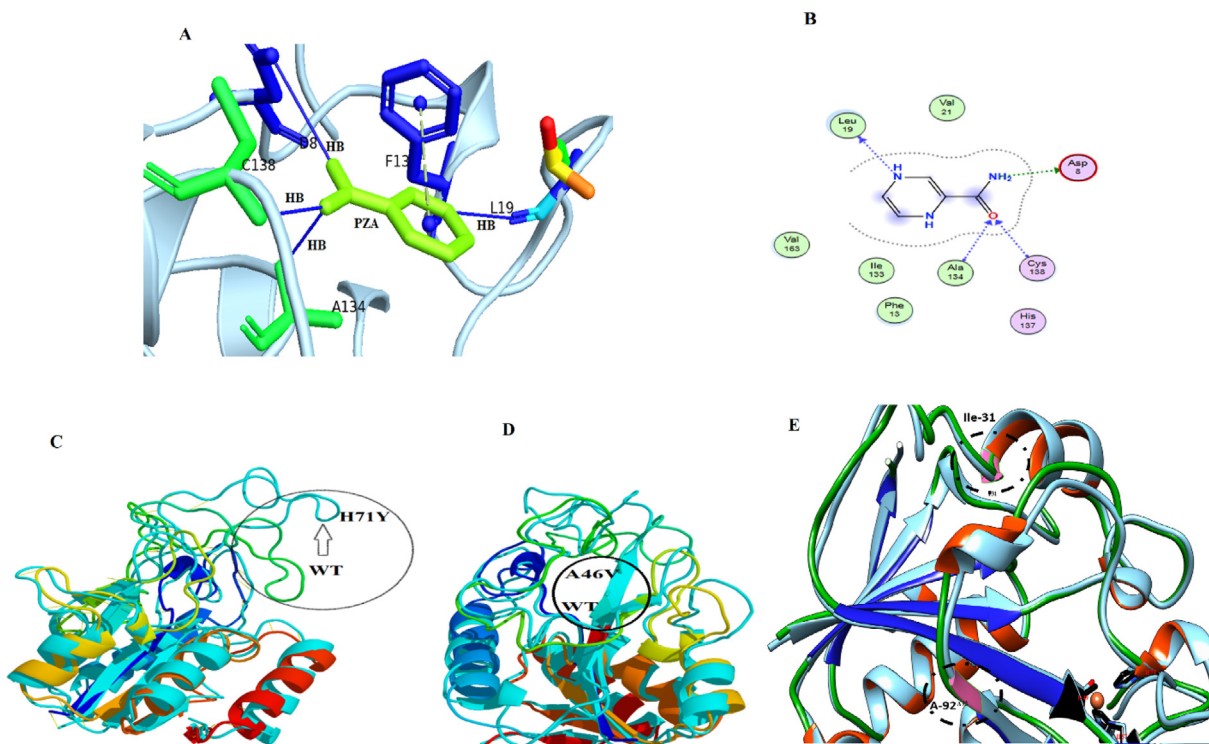
Fig. 1. PZA interactions with WT and MTs PZase. (A) The blue line indicates hydrogen bonding (HB). PZA binding pocket Residues C138, A134, E8, F13, and L19. (B) HB with D129N MTs and interaction with PZA. (C, D, E) MTs location and superimposition of MTs with WTs.

Fig. 2. RMSD of WT and MTs. WT and MTs attained noticeable alterations. WT is seemed to be stabled throughout the simulation while A46V, D129N, and H71Y exhibited high RMSD and more fluctuation (A). D129N exhibited very low RMSD (B).
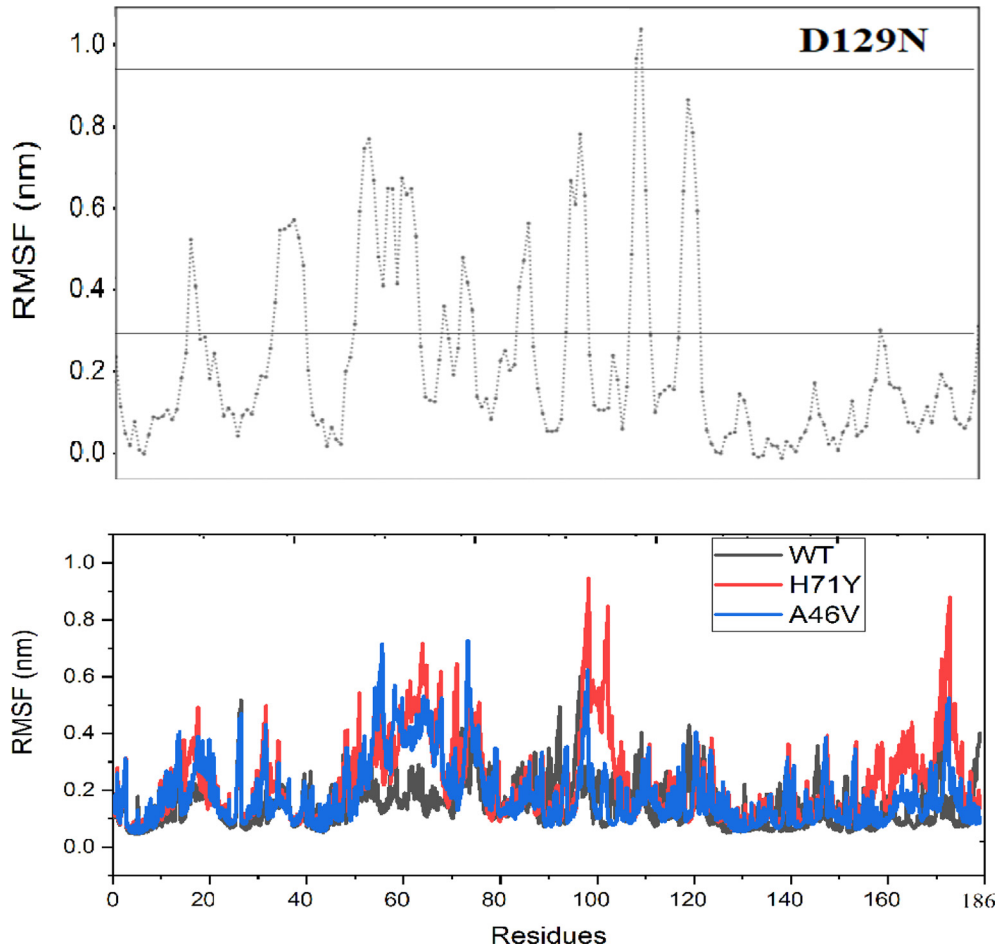
Fig. 3. RMSF comparison between WT and MTs. High RMSF has been observed in MTs at residues, 10–100 and 160–170.
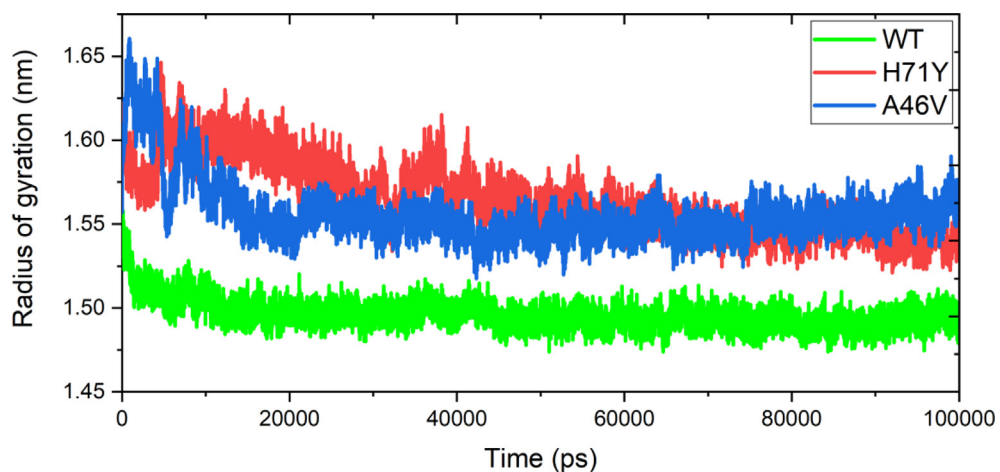

Fig. 4. Rg analysis of WT and MTs. A content or constant graph curve (green) shows a stable folding of WT as compared to MTs (red and blue. The folding effect of mutation may change the optimum catalytic activity of PZase to convert the pro-PZA into active form POA for the elimination of dormant MTB isolates.

shows conformational stability of WT. The Rg curves of A46V and H71Y seem to be more inconsistent.

4. Discussion

The rise of first- and second-line drug resistance is a foremost barrier towards the WHO plan of TB free world by 2035. The main first line of defense is the PZA drug that is highly useful in the execution of non-replicated MTB's subpopulations. Previous reports on the PZA resistance claimed that *pncA* gene mutations are responsible for the development of drug resistance. Nevertheless, in infrequent situations, it is observed that rpsA and aspartate decarboxylase (panD) genes mutation may also cause resistance to this first line of defense (Akhmetova et al., 2015; Shi et al.,

2014; Zhang et al., 2013). Recently we identified some novel mutations in the *pncA* gene that are PZA resistant isolated from the Northern areas (KP) of Pakistan. The data is uploaded to NCBI and can be accessed via the accession number MH461111-17 in the GeneBank. Though these novel mutations are identified and passed through several wet lab investigations that confirmed the resistance and importance of these mutations, the molecular mechanism behind these reported mutations A46V, D129N, and H71Y was still unveiled.

Amino acids define the 3D conformation of a protein which is crucial for the function. However, changes in the amino acid sequence may cause minor or major conformational drifts that could directly affect the protein's native function because the function of the protein is highly dependent upon the structure. These variations greatly affect the flexibility of a protein and this deviation from the native position could make it hard for the desired ligand to be bound. Since this directly affects the interactions that must be set up among these two entities. For all the mutations the RMSD and RMSF values of MTs A46V, D129N, and H71Y appeared to be more elevated in contrast to the WT which indicates a high level of instability. These outcomes agree with the previous reports (Junaid et al., 2018; Khan et al., 2019a, 2019b; Khan et al., 2018d) on PZase mutations (Fig. 4) (Aggarwal et al., 2017; He et al., 2018; Vats et al., 2015). It has been observed that that variation in the delicate site residues may not only modulate the allosteric site as well as change the dynamics of enzymes, resulting in drug resistance.

For a protein, its compactness and folding are highly important which is estimated via Rg that is the mass-weight root mean square distance of atomic assembly from a mutual point of mass, plotted against time (Fig. 4) (Lobanov et al., 2008; Smilgies and Folta-Stogniew, 2015). The Rg values depict the folding of MTs indicating an unstable pattern in comparison with WT that may be involved in weak interactions of PZase with PZA to convert it into active from POA. The protein folding instability and effect have already been investigated by Yoon et al (Yoon et al., 2014).

The binding pocket volume of PZase may directly affect the binding affinity with PZA. Pocket volume is considered optimum for a good binding affinity and any deviation in pocket volume may cause a weak or loss of interaction (Swier et al., 2017). Histidine at position 71 is an important interacting with metal ion present close to the binding pocket. Mutation H71Y may render a decrease in the pocket volume (Table 1). Coordination of metal ions and their interactions are important in metalloproteins that have physiological implications as well as structure, functional properties. From a molecular point, metal-binding may bring local constraints of protein flexibility which may produce long-range interactions as well as conformational effects (Dokmanić et al., 2008; Rotilio, 1980). Interaction of biomolecules with metals is fundamental in many cases for the constitution of active sites. In the current study, a metal ion effect has been observed that might be involved in conformational changes behind mutations (Fig. 5).

In conclusion mutations, A46V, H71Y, and D129N in PZase might be involved to alter its dynamic behavior for which the experimental results have already been provided. These mutations affect the PZase activity, flexibility, stability, and folding that offer weak or loss of PZA conversion activity into active form POA. Thus, this study may be used for better management of drug-resistant TB in the future.

CRediT authorship contribution statement

Muhammad Tahir Khan: Conceptualization, Formal analysis. **Sathishkumar Chinnasamy:** Data curation, Formal analysis. **Zhilei Cui:** . **Muhammad Irfan:** . **Dong-Qing Wei:** Conceptualization, Funding acquisition.

Declaration of Competing Interest

The authors declare that they have no known competing financial interests or personal relationships that could have appeared to influence the work reported in this paper.
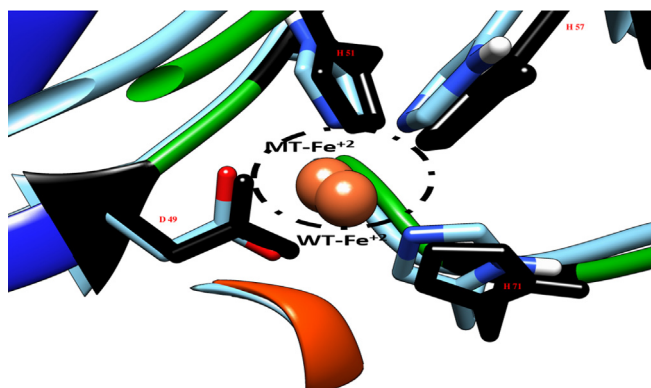
Acknowledgments

Funding

Fig. 5. Metal Fe^{+2} ion effect. Fe^{+2} of WT (black coordination residues) and MT. Residue D49N is deviated towards left, causing Fe^{+2} ion deviation from the original position. Although mutation occurs at far site beta-sheet 4 but the effect may be on the overall activity of an enzyme, interfering with biological function.

References

Aggarwal, M., Singh, A., Grover, S., Pandey, B., Kumari, A., Grover, A., 2017. Role of pnc A gene mutations W68R and W68G in pyrazinamide resistance. J. Cell. Biochem. 13, 593.

Akhmetova, A., Kozhamkulov, U., Bismilda, V., Chingissova, L., Abildaev, T., Dymova, M., Filipenko, M., Ramanculov, E., 2015. Mutations in the pncA and rpsA genes among 77 Mycobacterium tuberculosis isolates in Kazakhstan. Int. J. Tuberc. Lung Dis. 19, 179–184.

Alexander, D.C, Ma, J.H., Guthrie, J.L., Blair, J., Chedore, P., Jamieson, F.B., 2013. Reply to "Role of rpsA Gene Sequencing in Diagnosis of Pyrazinamide Resistance". J. Clin. Microbiol. 51, 383. https://doi.org/10.1128/JCM.02760-12.

Anand, R., 2018. Identification of potential antituberculosis drugs through docking and virtual screening. Interdiscip. Sci. Comput. Life Sci. 10, 419–429. https://doi.org/10.1007/s12539-016-0175-6.

Berendsen, H.J.C., van der Spoel, D., van Drunen, R., 1995. GROMACS: A message-passing parallel molecular dynamics implementation. Comput. Phys. Commun. 91, 43–56. https://doi.org/10.1016/0010-4655(95)00042-E.

Berman, H.M., 2008. The Protein Data Bank: a historical perspective. Acta Crystallogr. A 64, 88–95. https://doi.org/10.1107/S0108767307035623.

Bolton, E.E., Wang, Y., Thiessen, P.A., Bryant, S.H., 2008. Chapter 12 - PubChem: integrated platform of small molecules and biological activities. In: Wheeler, R. A., Spellmeyer, D.C. (Eds.), Annual Reports in Computational Chemistry. Elsevier, pp. 217–241.

Buck, G.E., O'Hara, L.C., Summersgill, J.T., 1992. Rapid, simple method for treating clinical specimens containing Mycobacterium tuberculosis to remove DNA for polymerase chain reaction. J. Clin. Microbiol. 30, 1331–1334.

Davies, A.P., Billington, O.J., McHugh, T.D., Mitchison, D.A., Gillespie, S.H., 2000. Comparison of phenotypic and genotypic methods for pyrazinamide susceptibility testing with Mycobacterium tuberculosis. J. Clin. Microbiol. 38, 3686–3688.

Ding, B., Li, N., Wang, W., 2013. Characterizing binding of small molecules. II. Evaluating the potency of small molecules to combat resistance based on docking structures. J. Chem. Inf. Model. 53, 1213–1222. https://doi.org/10.1021/ci400011c.

Dokmanić, I., Sikić, M., Tomić, S., 2008. Metals in proteins: correlation between the metal-ion type, coordination number and the amino-acid residues involved in the coordination. Acta Crystallogr. D Biol. Crystallogr. 64, 257–263. https://doi.org/10.1107/S090744490706595X.

Du, X., Wang, W., Kim, R., Yakota, H., Nguyen, H., Kim, S.-H., 2001. Crystal structure and mechanism of catalysis of a pyrazinamidase from Pyrococcus horikoshii. Biochemistry 40, 14166–14172.

Durairaj, D.R., Shanmughavel, P., 2019. In silico drug design of thiolactomycin derivatives against Mtb-KasA enzyme a route to inhibit multidrug resistance of Mycobacterium tuberculosis. Interdiscip. Sci. Comput. Life Sci. 11, 215–225. https://doi.org/10.1007/s12539-017-0257-0.

Ganesan, P., Ramalingam, R., 2018. Investigation of structural stability and functionality of homodimeric gramicidin towards peptide-based drug: a molecular simulation approach. J. Cell. Biochem. https://doi.org/10.1002/jcb.27765.

Haq, O., Andrec, M., Morozov, A.V., Levy, R.M., 2012. Correlated electrostatic mutations provide a reservoir of stability in HIV protease. PLOS Comput. Biol. 8,. https://doi.org/10.1371/journal.pcbi.1002675 e1002675.

He, M., Li, W., Zheng, Q., Zhang, H., 2018. A molecular dynamics investigation into the mechanisms of alectinib resistance of three ALK mutants. J. Cell. Biochem. 119, 5332–5342. https://doi.org/10.1002/jcb.26666.

Hou, T., McLaughlin, W.A., Wang, W., 2008. Evaluating the potency of HIV-1 protease drugs to combat resistance. Proteins 71, 1163–1174. https://doi.org/10.1002/prot.21808.

Junaid, M., Khan, M.T., Malik, S.I., Wei, D.-Q., 2018. Insights into the mechanisms of pyrazinamide resistance of three pyrazinamidase mutants N11K, P69T and D126N. J. Chem. Inf. Model. https://doi.org/10.1021/acs.jcim.8b00525.

Khan, M. Kalim A., Akhtar, S., Arif, J.M., 2018. Development of in silico protocols to predict structural insights into the metabolic activation pathways of xenobiotics. Interdiscip. Sci. Comput. Life Sci. 10, 329–345. Doi: 10.1007/s12539-017-0237-4.

Khan, Muhammad Tahir, Junaid, M., Mao, X., Wang, Y., Hussain, A., Malik, S.I., Wei, D.-Q., 2018a. Pyrazinamide resistance and mutations L19R, R140H, and E144K in Pyrazinamidase of Mycobacterium tuberculosis. J. Cell. Biochem. https://doi.org/10.1002/jcb.27989.

Khan, M.T., Khan, A., Rehman, A.U., Wang, Y., Akhtar, K., Malik, S.I., Wei, D.-Q., 2019a. Structural and free energy landscape of novel mutations in ribosomal protein S1 (rpsA) associated with pyrazinamide resistance. Sci. Rep. 9, 7482. https://doi.org/10.1038/s41598-019-44013-9.

Khan, M.T., Malik, S.I., Ali, S., Masood, N., Nadeem, T., Khan, A.S., Afzal, M.T., 2019. Pyrazinamide resistance and mutations in pncA among isolates of Mycobacterium tuberculosis from Khyber Pakhtunkhwa, Pakistan. BMC Infect. Dis. 19, 116. Doi: 10.1186/s12879-019-3764-2.

Khan, M.T., Malik, S.I., Ali, S., Sheed Khan, A., Nadeem, T., Zeb, M.T., Masood, N., Afzal, M.T., 2018b. Prevalence of pyrazinamide resistance in Khyber Pakhtunkhwa, Pakistan. Microb. Drug Resist. Larchmt. N. Doi: 10.1089/mdr.2017.0234.

Khan, M.T., Malik, S.I., Bhatti, A.I., Ali, S., Khan, A.S., Zeb, M.T., Nadeem, T., Fazal, S., 2018c. Pyrazinamide-resistant mycobacterium tuberculosis isolates from Khyber Pakhtunkhwa and rpsA mutations. J. Biol. Regul. Homeost. Agents 32, 705–709.

Khan, Muhammad Tahir, Rehaman, A.U., Junaid, M., Malik, S.I., Wei, D.-Q., 2018d. Insight into novel clinical mutants of RpsA-S324F, E325K, and G341R of Mycobacterium tuberculosis associated with pyrazinamide resistance. Comput. Struct. Biotechnol. J. Doi: 10.1016/j.csbj.2018.09.004.

Kirschner, P., Springer, B., Vogel, U., Meier, A., Wrede, A., Kiekenbeck, M., Bange, F.C., Böttger, E.C., 1993. Genotypic identification of mycobacteria by nucleic acid sequence determination: report of a 2-year experience in a clinical laboratory. J. Clin. Microbiol. 31, 2882–2889.

Kosloff, M., Kolodny, R., 2008. Sequence-similar, structure-dissimilar protein pairs in the PDB. Proteins 71, 891–902. https://doi.org/10.1002/prot.21770.

Kubica, G.P., Dye, W.E., Cohn, M.L., Middlebrook, G., 1963. Sputum digestion and decontamination with N-acetyl-L-cysteine-sodium hydroxide for culture of mycobacteria. Am. Rev. Respir. Dis. 87, 775–779. https://doi.org/10.1164/arrd.1963.87.5.775.

L DeLano, W., 2002. The PyMOL Molecular Graphics System (2002) DeLano Scientific, Palo Alto, CA, USA. http://www.pymol.org.

Lemaitre, N., Callebaut, I., Frenois, F., Jarlier, V., Sougakof, W., 2001. Study of the structure–activity relationships for the pyrazinamidase (PncA) from Mycobacterium tuberculosis. Biochem. J. 353, 453–458.

Liu, H., Yao, X., 2010. Molecular basis of the interaction for an essential subunit PA-PB1 in influenza virus RNA polymerase: insights from molecular dynamics simulation and free energy calculation. Mol. Pharm. 7, 75–85. https://doi.org/10.1021/mp900131p.

Lobanov, M.Y., Bogatyreva, N.S., Galzitskaya, O.V., 2008. Radius of gyration as an indicator of protein structure compactness. Mol. Biol. 42, 623–628. https://doi.org/10.1134/S0026893308040195.

Lu, P., Haagsma, A.C., Pham, H., Maaskant, J.J., Mol, S., Lill, H., Bald, D., 2011. Pyrazinoic acid decreases the proton motive force, respiratory ATP synthesis activity, and cellular ATP levels. Antimicrob. Agents Chemother. 55, 5354–5357. https://doi.org/10.1128/AAC.00507-11.

Ma, B., Elkayam, T., Wolfson, H., Nussinov, R., 2003. Protein-protein interactions: structurally conserved residues distinguish between binding sites and exposed protein surfaces. Proc. Natl. Acad. Sci. USA 100, 5772–5777. https://doi.org/10.1073/pnas.1030237100.

Njire, M., Tan, Y., Mugweru, J., Wang, C., Guo, J., Yew, W., Tan, S., Zhang, T., 2016. Pyrazinamide resistance in Mycobacterium tuberculosis: review and update. Adv. Med. Sci. 61, 63–71. https://doi.org/10.1016/j.advms.2015.09.007.

Petrella, S., Gelus-Ziental, N., Maudry, A., Laurans, C., Boudjelloul, R., Sougakoff, W., 2011. Crystal structure of the pyrazinamidase of Mycobacterium tuberculosis: insights into natural and acquired resistance to pyrazinamide. PLoS One 6, e15785.

Pettersen, E.F., Goddard, T.D., Huang, C.C., Couch, G.S., Greenblatt, D.M., Meng, E.C., Ferrin, T.E., 2004. UCSF Chimera–a visualization system for exploratory research and analysis. J. Comput. Chem. 25, 1605–1612. https://doi.org/10.1002/jcc.20084.

Rehman, A.U., Khan, M.T., Liu, H., Wadood, A., Malik, S.I., Chen, H.-F., 2019. Exploring the pyrazinamide drug resistance mechanism of clinical mutants T370P and W403G in ribosomal protein S1 of Mycobacterium tuberculosis. J. Chem. Inf. Model. 59, 1584–1597. https://doi.org/10.1021/acs.jcim.8b00956.

Rotilio, G., 1980. Interaction of metal ions with proteins: an overview. Inorg. Chim. Acta 40, X49. https://doi.org/10.1016/S0020-1693(00)92105-4.

Sheen, P., Ferrer, P., Gilman, R.H., López-Llano, J., Fuentes, P., Valencia, E., Zimic, M.J., 2009. Effect of pyrazinamidase activity on pyrazinamide resistance in Mycobacterium tuberculosis. Tuberculosis 89, 109–113.

Shi, W., Chen, J., Feng, J., Cui, P., Zhang, S., Weng, X., Zhang, W., Zhang, Y., 2014. Aspartate decarboxylase (PanD) as a new target of pyrazinamide in Mycobacterium tuberculosis. Emerg. Microbes Infect. 3, e58.

Siddiqi, S.H., Gerdes, S.R., 2006. Foundation for Innovative New Diagnostics (FIND) MGITTM Procedure Manual for BACTEC™ MGIT 960™ TB System. Switzerland.

Simons, S.O., Mulder, A., van Ingen, J., Boeree, M.J., van Soolingen, D., 2013. Role of rpsA gene sequencing in diagnosis of pyrazinamide resistance. J. Clin. Microbiol. 51.

Smilgies, D.-M., Folta-Stogniew, E., 2015. Molecular weight–gyration radius relation of globular proteins: a comparison of light scattering, small-angle X-ray scattering and structure-based data. J. Appl. Crystallogr. 48, 1604–1606. https://doi.org/10.1107/S1600576715015551.

Sørensen, M.A., Fricke, J., Pedersen, S., 1998. Ribosomal protein S1 is required for translation of most, if not all, natural mRNAs in Escherichia coli in vivo11Edited by D. Draper. J. Mol. Biol. 280, 561–569. https://doi.org/10.1006/jmbi.1998.1909.

Stehr, M., Elamin, A., Singh, M., 2015. Pyrazinamide: the importance of uncovering the mechanisms of action in mycobacteria. Expert Rev. Anti Infect. Ther. 13, 593–603.

Swier, L.J.Y.M., Monjas, L., Reeßing, F., Oudshoorn, R.C., Aisyah, Primke, T., Bakker, M.M., Olst, E. van, Ritschel, T., Faustino, I., Marrink, S.J., Hirsch, A.K.H., Slotboom, D.J., 2017. Insight into the complete substrate-binding pocket of ThiT by chemical and genetic mutations. MedChemComm 8, 1121–1130. Doi: 10.1039/C7MD00079K.

Tan, Y., Hu, Z., Zhang, T., Cai, X., Kuang, H., Liu, Y., Chen, J., Yang, F., Zhang, K., Tan, S., 2014. Role of pncA and rpsA gene sequencing in detection of pyrazinamide resistance in Mycobacterium tuberculosis isolates from southern China. J. Clin. Microbiol. 52, 291–297.

Vats, C., Dhanjal, J., Goyal, S., Gupta, A., Bharadvaja, N., Grover, A., 2015. Mechanistic analysis elucidating the relationship between Lys96 mutation in Mycobacterium tuberculosis pyrazinamidase enzyme and pyrazinamide susceptibility. BMC Genomics 16 (Suppl 2), S14. https://doi.org/10.1186/1471-2164-16-S2-S14.

World Health Organization, 2018. Global tuberculosis report 2018. World Health Organization, S.l.

Worth, C.L., Gong, S., Blundell, T.L., 2009. Structural and functional constraints in the evolution of protein families. Nat. Rev. Mol. Cell Biol. 10, 709–720. https://doi.org/10.1038/nrm2762.

Wu, Y., Tepper, H., Voth, G., J, 2006. Flexible simple point-charge water model with improved liquid-state properties. Phys 024503 124 SRC-GoogleScholar.

Xue, W., Pan, D., Yang, Y., Liu, H., Yao, X., 2012. Molecular modeling study on the resistance mechanism of HCV NS3/4A serine protease mutants R155K, A156V and D168A to TMC435. Antiviral Res. 93, 126–137. https://doi.org/10.1016/j.antiviral.2011.11.007.

Yadon, A.N., Maharaj, K., Adamson, J.H., Lai, Y.-P., Sacchettini, J.C., Ioerger, T.R., Rubin, E.J., Pym, A.S., 2017. A comprehensive characterization of PncA polymorphisms that confer resistance to pyrazinamide. Nat. Commun. 8. https://doi.org/10.1038/s41467-017-00721-2.

Yang, J., Liu, Y., Bi, J., Cai, Q., Liao, X., Li, W., Guo, C., Zhang, Q., Lin, T., Zhao, Y., Wang, H., Liu, J., Zhang, X., Lin, D., 2015. Structural basis for targeting the ribosomal protein S1 of Mycobacterium tuberculosis by pyrazinamide. Mol. Microbiol. 95, 791–803. https://doi.org/10.1111/mmi.12892.

Ying, Z., Wade, M.M., Scorpio, A., Zhang, H., Sun, Z., 2003. Mode of action of pyrazinamide: disruption of Mycobacterium tuberculosis membrane transport and energetics by pyrazinoic acid. J. Antimicrob. Chemother. 52, 790–795.

Yoon, J.-H., Nam, J.-S., Kim, K.-J., Ro, Y.-T., 2014. Characterization of pncA mutations in pyrazinamide-resistant Mycobacterium tuberculosis isolates from Korea and analysis of the correlation between the mutations and pyrazinamidase activity. World J. Microbiol. Biotechnol. 30, 2821–2828.

Zhang, S., Chen, J., Shi, W., Liu, W., Zhang, W., Zhang, Y., 2013. Mutations in panD encoding aspartate decarboxylase are associated with pyrazinamide resistance in Mycobacterium tuberculosis. Emerg. Microbes Infect. 2, e34.